Bull Volcanol (2012) 74:2353–2362
DOI 10.1007/s00445-012-0667-0

RESEARCH ARTICLE

Time-lapse camera observations of gas piston activity at Pu‘u ‘Ō‘ō, Kīlauea volcano, Hawai‘i

Tim R. Orr · James C. Rea

Received: 9 June 2012 / Accepted: 23 September 2012 / Published online: 2 October 2012

Abstract Gas pistoning is a type of eruptive behavior described first at Kīlauea volcano and characterized by the (commonly) cyclic rise and fall of the lava surface within a volcanic vent or lava lake. Though recognized for decades, its cause continues to be debated, and determining why and when it occurs has important implications for understanding vesiculation and outgassing processes at basaltic volcanoes. Here, we describe gas piston activity that occurred at the Pu‘u ‘Ō‘ō cone, in Kīlauea's east rift zone, during June 2006. Direct, detailed measurements of lava level, made from time-lapse camera images captured at close range, show that the gas pistons during the study period lasted from 2 to 60 min, had volumes ranging from 14 to 104 m^3, displayed a slowing rise rate of the lava surface, and had an average gas release duration of 49 s. Our data are inconsistent with gas pistoning models that invoke gas slug rise or a dynamic pressure balance but are compatible with models which appeal to gas accumulation and loss near the top of the lava column, possibly through the generation and collapse of a foam layer.

Keywords Pu‘u ‘Ō‘ō · Kīlauea · Hawai‘i · Gas piston · Gas slug

Editorial responsibility: S. Calvari

Electronic supplementary material The online version of this article (doi:10.1007/s00445-012-0667-0) contains supplementary material, which is available to authorized users.

T. R. Orr (✉) · J. C. Rea
Hawaiian Volcano Observatory, U.S. Geological Survey,
Hawaii National Park, HI 96718, USA
e-mail: torr@usgs.gov

T. R. Orr
Department of Geology and Geophysics, University of Hawai‘i,
Honolulu, HI 96822, USA

Introduction

Gas pistoning—a type of lava-level fluctuation that occurs within a volcanic vent or lava lake and is often cyclic—has long been recognized at Kīlauea volcano (Swanson et al. 1971, 1979; Tilling et al. 1987; Wolfe et al. 1988; Ferrazzini et al. 1991; Barker et al. 2003; Johnson et al. 2005; Marchetti and Harris 2008; Patrick et al. 2011a, b). Gas piston activity was defined originally by Swanson et al. (1971), from observations made during the 1969–1971 Mauna Ulu eruption, as a cyclic process characterized by a slow rise of a relatively crusted lava surface followed by an abrupt drop in lava level accompanied by the ejection of pyroclasts (referred to here as the rise phase and gas release phase, respectively).

Four models have been proposed to explain this behavior. (1) In the crust-controlled gas accumulation model, gas is trapped beneath a relatively impermeable crust or viscous layer at the top of a lava column or lava lake and is released episodically (e.g., Swanson et al. 1971, 1979; Patrick et al. 2011a, b). In contrast, (2) the slug model invokes discrete gas slugs that form episodically and rise in the conduit and burst through the surface (e.g., Jaupart and Vergniolle 1988; Ferrazzini et al. 1991; Vergniolle and Mangan 2000; Edmonds and Gerlach 2007), and (3) the pressure balance model requires continuous streaming of gas which temporarily reduces the bulk density of the lava column, causing it to rise. Eventually, the system becomes unstable, the lava surface falls, and the system is reset for the next cycle to begin (Witham et al. 2006). Finally, (4) Dibble (1972) proposed a foam model for gas pistoning, suggesting that the behavior was caused by the formation and collapse of a foam layer at the top of a column of lava irrespective of the surface crust. In most situations, geologic observations and geophysical data are incapable of supporting one mechanism over the others (Marchetti and Harris 2008).

Patrick et al. (2011b) used time-lapse camera images from a distance of about 2 km to measure changes in lava level associated with gas piston activity in a broad, slowly moving channelized lava flow in Kīlauea's east rift zone. The form of the lava channel was much like that of a perched lava pond. Likewise, Patrick et al. (2011a) used webcam images from a distance of a few hundred meters to measure lava level changes in a 70-m-wide active lava lake at Kīlauea's summit. Using a similar technique, this study confirms their basic results but differs in that we directly observed gas pistoning at close range (meters) within a narrow vent. Because the vent was cylindrical, and in most cases the lava remained confined to the vent, we do not have to account for changes in vent width when quantifying changes in lava level. Our results provide additional constraints that improve our understanding of this cyclic behavior.

Throughout the text, we interchangeably use the terms *gas pistoning* and *gas piston activity* to refer to the cyclic behavior of lava level rise and fall as described above. We use the term *gas piston* to refer to a single cycle of rise and fall during gas pistoning.

Background

The Puʻu ʻŌʻō vent, located in the middle part of Kīlauea's subaerial east rift zone, has been erupting nearly continuously since 1983. During its first 3 years, the eruption was characterized by a series of episodic high lava fountains that built the 255-m-high pyroclastic cone of Puʻu ʻŌʻō (Wolfe et al. 1988; Heliker et al. 2003). Gas pistoning was frequently observed within the Puʻu ʻŌʻō vent conduit during the relatively quiet repose periods between the lava fountains (Wolfe et al. 1988).

In 1986, the focus of activity shifted to a new location about 3 km farther downrift, where nearly continuous effusion built the low Kupaianaha lava shield, holding a small lava lake, and transported lava downslope to form a broad, tube-fed pāhoehoe flow field (Mattox et al. 1993; Hon et al. 1994; Heliker and Mattox 2003). The summit of the Puʻu ʻŌʻō cone collapsed and widened progressively during this period, forming a crater that also often contained a small lava lake (Heliker et al. 1998, 2003). Gas pistoning occurred sporadically at both the Puʻu ʻŌʻō (e.g., Ferrazzini et al. 1991) and Kupaianaha (unpublished USGS data) lava lakes during this period.

The eruption changed again in 1992, when the Kupaianaha vent died and lava began to erupt from a succession of vents on the southwestern flank of the Puʻu ʻŌʻō cone (Kauahikaua et al. 1996; Heliker et al. 1998; Heliker and Mattox 2003). Over the following 15 years, the western and southern flanks of Puʻu ʻŌʻō were gradually buried beneath a lava shield, and lava flowed downslope most of the time, widening the existing tube-fed pāhoehoe flow field (Heliker and Mattox 2003). Outgassing vents, and sometimes small lava lakes, were present on the floor of the Puʻu ʻŌʻō crater throughout this interval, and periods of gas pistoning were routinely observed (e.g., Barker et al. 2003; Johnson et al. 2005; Marchetti and Harris 2008).

One such period was during March–October 2006, when gas pistoning occurred repeatedly at the informally named Drainhole vent (Figs. 1, 2, and 3, Online Resources 1 and 2), within a small pit on the edge of a larger collapse depression on the floor of the Puʻu ʻŌʻō crater (Fig. 2). The crater floor was at an altitude of ~860 m, or about 140 m above the pre-eruption ground surface and 210 m above the top of the magma storage body beneath Puʻu ʻŌʻō as modeled by gravity data (Heliker et al. 2003). Johnson et al. (2005) and Marchetti and Harris (2008) documented hundreds of gas pistons at this and other vents in Puʻu ʻŌʻō from 2001 to 2003. Comparable to what they observed, the gas release that ended each gas piston at the Drainhole vent during our study was accompanied by the ejection of pyroclasts (Fig. 3e, Online Resource 2) and followed by a pronounced gas release (Fig. 3f, Online Resource 2). In the 3 years between their observations and those presented here, the crater underwent additional filling, followed by a period of small-scale, episodic collapse that resulted in the formation of new pits on the crater

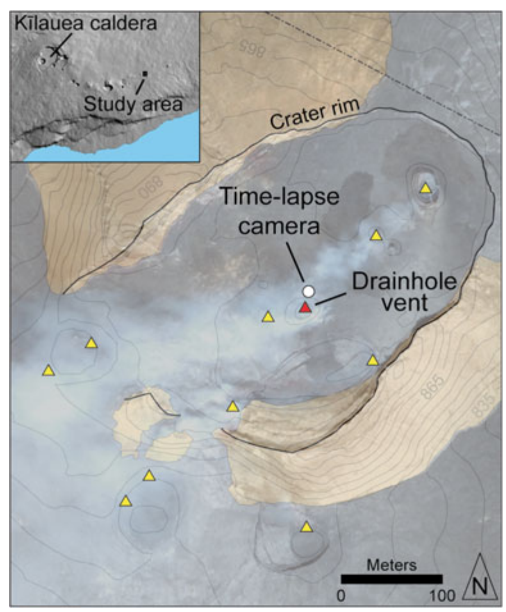

Fig. 1 Map of Puʻu ʻŌʻō cone and crater. Lava flows shown in *gray*; cone tephra shown in *brown*. *Red triangle* shows position of Drainhole vent. *Yellow triangles* show other active vents. *White circle* shows location of time-lapse camera deployment. Contour interval 5 m. *Inset*—map showing study area in relation to summit and upper east rift zone of Kīlauea Volcano

floor. The Drainhole vent was one of several vents that persisted, though with major modification, through these changes.

Data collection

A time-lapse camera system utilizing a Nikon Coolpix 4300 digital camera (Orr and Hoblitt 2008) was deployed on the north edge of the Drainhole pit, on the floor of the Puʻu ʻŌʻō crater, from June 2 to 8, 2006 (Fig. 2). The time-lapse camera was inclined 26° (±1°) below horizontal with a view into the vent and was programmed to capture one image per minute with a pixel resolution of 1,600×1,200.

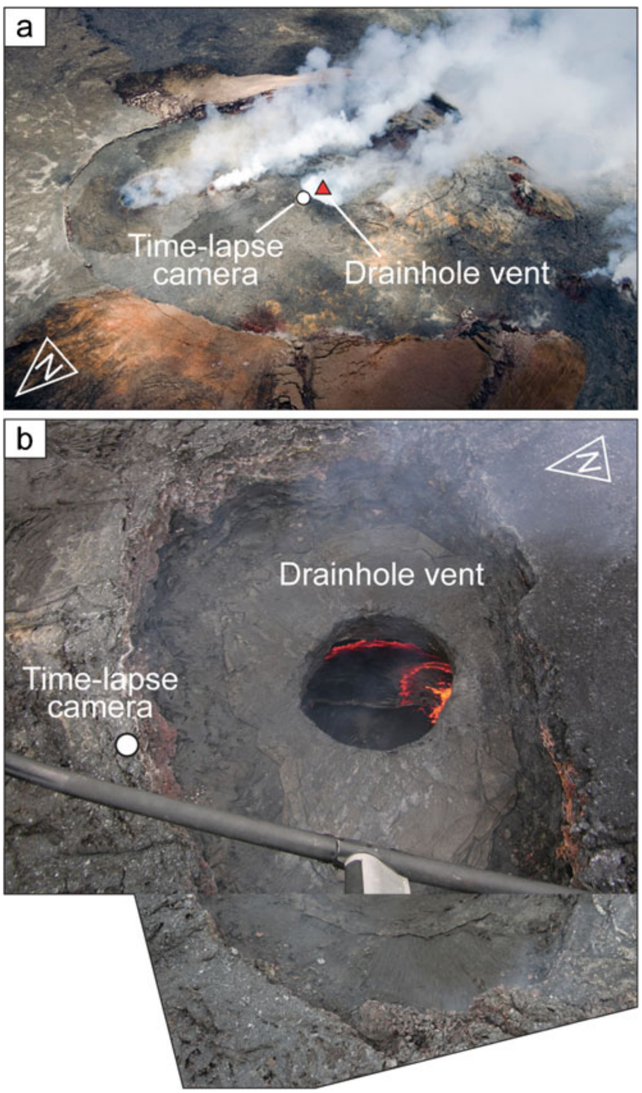

Fig. 2 **a** Oblique aerial photograph looking SSE showing configuration of vents on Puʻu ʻŌʻō crater floor, including Drainhole vent, on July 14, 2006. **b** Composite of two oblique aerial photographs looking E at Drainhole pit and vent. *White circle* designates location of time-lapse camera. Drainhole vent opening ~5 m diameter; Drainhole pit ~15 m across and ~30 m long. Upper photo from June 16, 2006; lower photo from July 21, 2006

During the camera deployment, the Drainhole pit was floored by relatively smooth pāhoehoe lava. The Drainhole vent was a ~5-m-diameter circular opening (±0.5 m) in the pit floor, and the walls of the vent visible within this opening were nearly vertical (Figs. 2 and 3). During periods without gas pistoning, the top of the lava column was sometimes just above, and sometimes just below, the lowest point visible in the vent as viewed from the position of the time-lapse camera. Between individual gas pistons during periods of cyclic activity, the lava surface was, in nearly every case, slightly too deep to be seen from the ground (Fig. 3a). From the air, when the lava surface was at a low level during periods without gas pistoning, the walls of the vent appeared to widen abruptly several meters below the opening, just above the lava surface (Fig. 2b), suggesting that the floor of the Drainhole pit formed a roof over a small lava lake. This was shown to be the case when the floor of the pit later collapsed. The point at which the vent walls widened to form the lava lake roof was below the level visible to the time-lapse camera, and the lava rise associated with gas pistoning was confined essentially to the narrow cylindrical part of the vent above this flare. The horizontal distance between the camera position and the opposite side of the vent, along the center line of the camera's field of view, was ~11 m (±1 m).

The time-lapse camera images were used to document the lava surface rise duration, maximum height, and gas release duration of all measurable gas pistons during the deployment period. Rise durations were measured from the first time-lapse frame in which the lava surface was seen to be rising, to the last frame before gas release had begun or the lava surface was seen to have dropped out of sight. Gas release duration was simply recorded as the number of images (0, 1, or 2) that captured some part of the falling and disrupted lava surface prior to the heavy gas emission that we take as the end of the gas piston. A statistical analysis was then performed on the gas release duration data to determine an average duration.

The position of the lava surface within the Drainhole vent was measured for each frame for a subset of 40 gas pistons. In each case, the y pixel coordinate, measured from the bottom of the image to the intersection of the lava surface with the near-vertical wall of the vent opposite the camera, was recorded along the vertical center line of the image. Measurement accuracy in most cases is thought to be ±2 pixels, but could be ±10 pixels in rare cases when visibility was poor. Because the time-lapse camera was inclined, the y pixel value measured from each time-lapse image represented the height of the lava column as projected onto a plane perpendicular to the center line of the camera's field

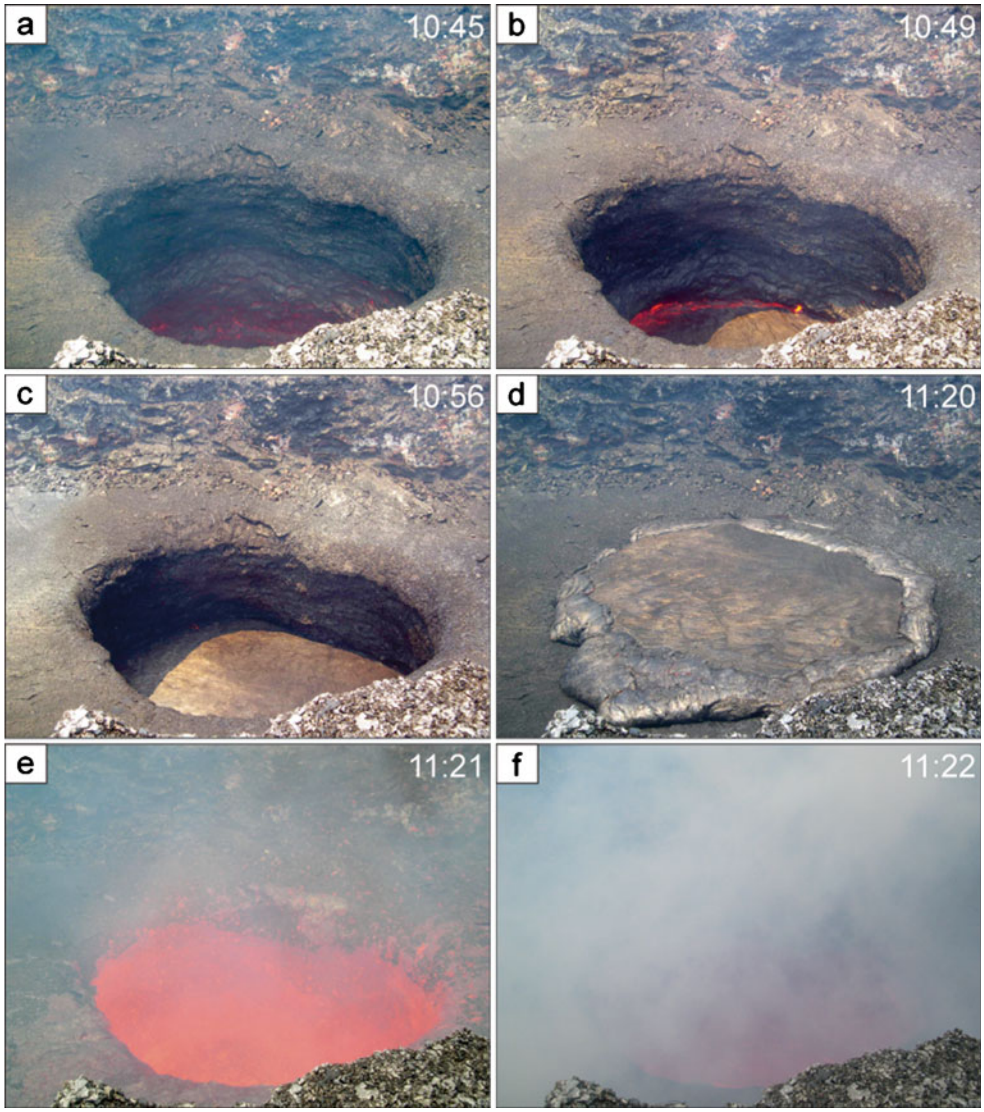

Fig. 3 Time-lapse images showing single gas piston cycle spanning period from 10:45 to 11:22 local time on June 3, 2006. Gas piston also included in movie shown in Online Resource 2. Width of vent opening ~5 m. **a** Lava surface at background level just below field of view. **b–c** Lava surface rising. **d** Lava surface reaches highest level and overflows vent rim. **e** Lava surface dropping abruptly, accompanied by bright incandescence and ejection of pyroclasts. **f** Pronounced gas release marks end of gas piston

of view, i.e., perpendicular to a line with a slope of 26°. To calculate the actual lava surface position, it was necessary to re-project the lava surface to the vertical plane defined by the vent wall (Appendix).

Time-lapse camera images were also used to quantify changes in vent brightness over time within the Drainhole vent for a sequence of seven gas pistons to compare with other observations of gas pistoning using similar data (Johnson et al. 2005; Edmonds and Gerlach 2007; Marchetti and Harris 2008; Patrick et al. 2011a). To perform this analysis, a MATLAB (version 2009b, ® The Mathworks, Inc.) routine, modified from that described by Patrick et al. (2010), converted the individual time-lapse images from color to grayscale and calculated a unitless mean brightness value within a static observation window 100 pixels wide and 700 pixels high placed over the vent opening along the vertical center line of each image.

Results

There were 219 measurable gas pistons recorded at the Drainhole vent during the 6-day deployment period. Dozens of other gas pistons occurred but were too small to be quantified and are excluded. The rise phase of the gas pistons ranged in duration from 2 to 60 min (Fig. 4b) with a mean of 13 min. The rise phase was characterized by the formation of a crust on the lava surface that resulted in a decrease in vent incandescence. The duration of the gas release phase could not be measured precisely because of the 1-min time-lapse interval. In most instances, the gas release was captured by only one time-lapse image frame. In other cases, the gas release occurred entirely between frames (i.e., the lava surface was visible at a high stand in one frame but had dropped completely out of sight by the next), indicating that the gas release lasted for less than 1 min. In a few instances, the gas release was recorded in

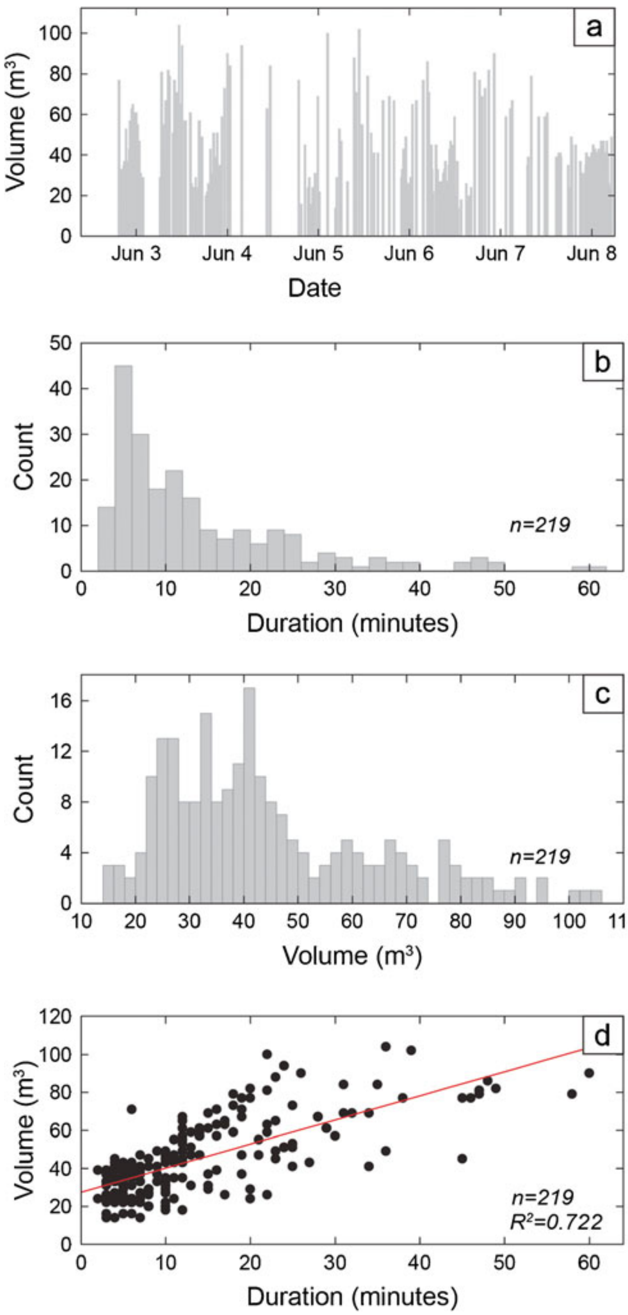

Fig. 4 **a** Plot showing gas piston occurrence and volume for the study period. **b** Histogram showing duration of gas pistons recorded at Drainhole vent. **c** Histogram showing volume of gas pistons recorded at Drainhole vent. **d** Scatter plot showing roughly linear relation between duration and volume of gas pistons at Drainhole vent

two sequential frames, indicating that it lasted for longer than 1 min. The statistical analysis performed on these data, considering the relative numbers of instances where the gas release was recorded in 0, 1, or 2 frames (52, 152, and 15 instances, respectively), suggests an average gas release duration of 49 s. The gas pistons also occurred typically in clusters (Fig. 4a), often with no time gap between individual events discernible by the 1-min time-lapse interval. Furthermore, there was no discernible pattern among the durations of successive gas piston cycles. A gas piston lasting several tens of minutes was commonly preceded or followed immediately by one lasting only a few minutes.

The measured gas pistons ranged in height from 0.7 m to 5.3 m above the lowest visible point in the vent. Approximating the Drainhole vent as a vertical cylindrical conduit 5 m in diameter, these heights translate to volumes ranging from 14 to 104 m^3 (Fig. 4c). In most cases, these are minimum volumes because the lava surface fell an estimated 1–2 m below the lowest visible point in the vent at the end of each gas piston. To determine gas mass, we first use the ideal gas law to calculate gas density:

$$\rho = \frac{P}{RT} \tag{1}$$

where ρ is gas density, P is pressure, R is the specific gas constant, and T is the gas temperature. It is assumed that the gas is at magmatic temperature (1,145 °C for lava erupted at Puʻu ʻŌʻō at this time; unpublished USGS data), composed entirely of water vapor (R=462 $\mathrm{Jkg^{-1}K^{-1}}$), and near the surface where pressure may be approximated as atmospheric (9×10^4Pa at 860 m altitude). This produces a gas density of 0.17 $\mathrm{kgm^{-3}}$ which, when multiplied by the volume change, yields rough minimum gas masses ranging from 2 to 18 kg. If we assume a maximum overburden thickness of 0.2 m just before the gas release phase of the gas piston (a reasonable thickness based on the time-lapse camera images) and an overburden density of 1,000 $\mathrm{kgm^{-1}}$ (reasonable for near-vent lava; Cashman et al. (1994)), the gas mass is not significantly increased. In general, the rise phase of the largest gas pistons observed in this study (i.e., those with the largest gas volume and mass) had the longest duration. This is illustrated in Fig. 4d, which shows a rough linear relation between gas piston volume and duration.

In most cases, the amount of lava level rise between each successive time-lapse frame for a particular gas piston decreased as the lava surface approached its highest level (Fig. 5). This implies a deceleration of the rising lava surface. For those gas pistons that did not show a distinct decrease in the lava surface rise rate—generally restricted to short-duration events—the lava surface height increased more or less linearly. In no case is there an indication of a prolonged increasing rise distance between time-lapse frames that would suggest an acceleration of the lava surface.

The quantification of changes in vent brightness during gas pistoning also revealed a direct relation with lava level rise. Specifically, the slowing rate of lava level rise mirrored the slowing rate of decreasing vent brightness, as did the

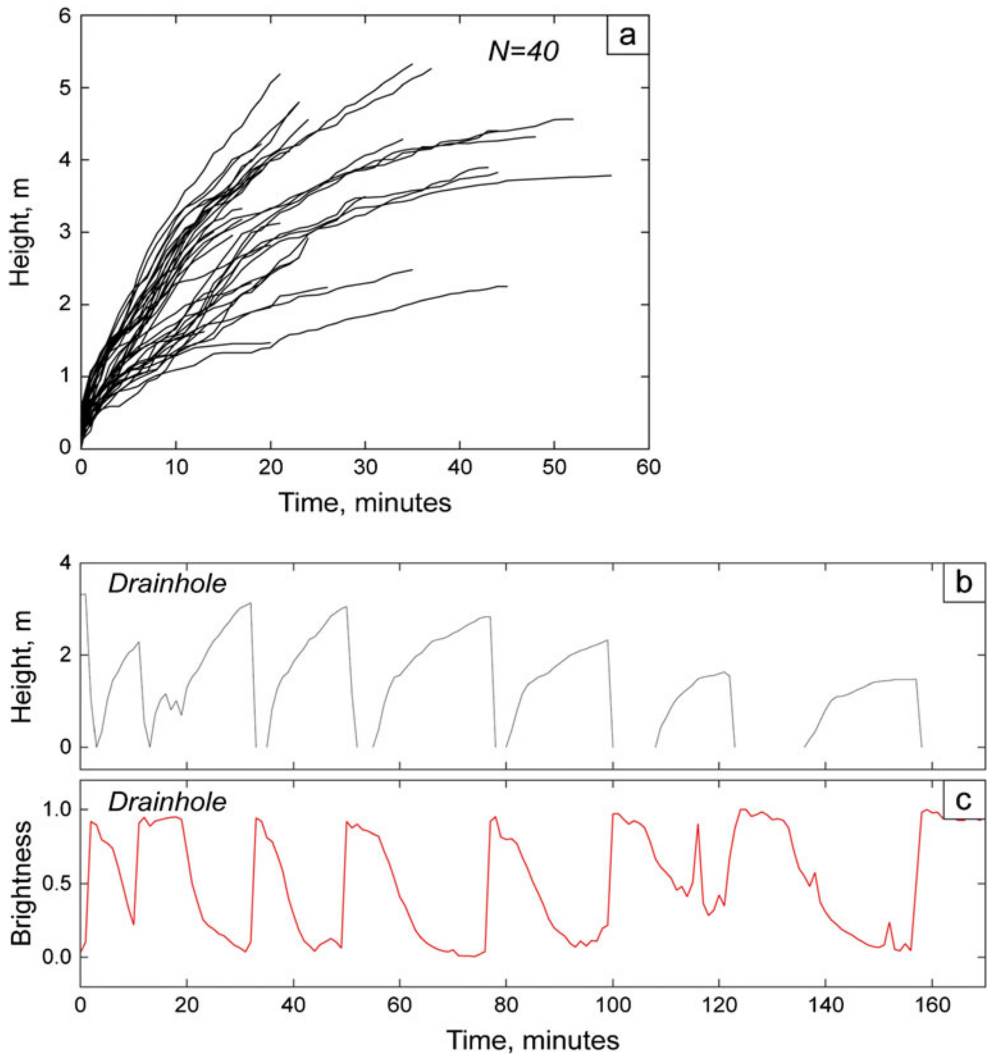

Fig. 5 **a** Line plot showing lava level through time for selected gas pistons at Drainhole vent. **b** Line plot showing lava level for 170-min sequence of seven gas pistons at Drainhole vent spanning 23:20 on June 2, 2006 to 02:00 on June 3, 2006. Zero height value represents deepest view into vent from time-lapse camera perspective. Sequence included in movie shown in Online Resource 1. **c** Line plot showing vent brightness over time for same gas piston sequence shown in (**b**)

abrupt drop in lava level and the abrupt increase in brightness at the end of each gas piston (Fig. 5b).

Discussion

Because most CO_2 is lost at Kīlauea's summit, H_2O and SO_2 are the dominant components of the volcanic plume emitted at Puʻu ʻŌʻō, with H_2O far exceeding SO_2 (Gerlach and Graeber 1985). Despite the paucity of SO_2 compared to H_2O, approximately 2,000 metric tons of SO_2 per day were released from Puʻu ʻŌʻō during June 2006 (Elias and Sutton 2007). Nearly all H_2O and SO_2 exsolution occurs within 150 m of the surface (Gerlach 1986), which means that these volatiles are exsolving primarily within the narrow conduits that connect the magma body beneath Puʻu ʻŌʻō to the surface, or within shallower zones of magma storage within the Puʻu ʻŌʻō edifice as expressed by the presence of nested pits on the crater floor. Thus, shallow outgassing behavior at Puʻu ʻŌʻō is controlled by these two gas species, and dominantly by H_2O. Because gas pistoning can be a common mode of outgassing for long intervals (weeks to months), it is likely controlled by outgassing of the dominant gas species.

The gas release phase of gas pistons is often described as being abrupt (e.g., Wolfe et al. 1988; Barker et al. 2003), which is often interpreted as occurring over a time scale typically associated with Strombolian bursts. For example, the gas release during explosions at Stromboli lasts an average of 15 s (Patrick et al. 2007), while gas bursts at Erebus, even including the rise of the lava surface, last only a few seconds (Dibble et al. 2008; Gerst et al. 2008). The volume change during gas pistoning at the Drainhole vent is of the same order of magnitude as the volume estimated for gas bursts at Stromboli volcano (Ripepe and Marchetti 2002) and similar in magnitude to the volume of the bubbles responsible for Strombolian bursts at Erebus (Aster et al. 2003). By comparison, though, the gas release during the gas pistoning documented here lasted 49 s, on average. This is consistent with the 1–2-min gas release duration reported by Swanson et al. (1979) for gas pistoning at Mauna Ulu and by Patrick et al. (2011a) for gas pistoning at Kīlauea's summit in 2009. The 1–2-min gas release duration is also consistent with other direct observations of gas piston activity at Kīlauea's summit in 2008 and 2009 and at Puʻu ʻŌʻō and Kupaianaha (unpublished USGS data). Our observations of the progression of the gas release phase agree with earlier ones (e.g., Swanson et al. 1979; Patrick et al. 2011a; unpublished USGS data), finding that the gas release begins with weak bubbling that quickly escalates and is accompanied by a lowering of the lava surface over the same duration as the gas release.

The gas mass released from the Drainhole vent during gas pistoning reported here is also on the same order of magnitude as gas slugs modeled by James et al. (2008), who showed that the lava surface above a rising gas slug should begin to increase in height only seconds to a few tens of seconds before the slug reaches the surface. Furthermore, lava surface height should increase exponentially (accelerate) during this brief period. Those results are inconsistent with the results obtained in this study, which show a rise duration two to three orders of magnitude longer, during which there was a deceleration of the rising lava surface. Combining a reasonable gas slug ascent velocity of 2 ms^{-1} (calculated from equation 8 of James et al. 2008) with even the shortest lava-surface-rise duration of 2 min implies an initial slug depth of 240 m—roughly consistent with the depth of the magma storage body beneath Puʻu ʻŌʻō but deeper than most H_2O and SO_2 exsolution and too deep to result in a concurrent lava level change at the surface. Temporary trapping of a gas slug in the shallow lava body directly beneath the floor of the Drainhole pit can be ruled out because gas pistoning continued to occur in the Drainhole vent following collapse of the pit floor days after the period studied here. These later gas pistons, though larger in amplitude and occurring in a larger diameter body of lava, were of similar duration and followed the same trends of slowing rise rate as the gas pistons we analyzed (unpublished USGS data).

Like other slug-driven models for gas pistoning (e.g., Jaupart and Vergniolle 1988; Ferrazzini et al. 1991; Vergniolle and Mangan 2000; Edmonds and Gerlach 2007), the model of Johnson et al. (2005) envisions lava pushed upward ahead of an ascending gas slug. Johnson et al. (2005) build upon the gas slug model by proposing that, for the gas release to commence, the lava above the slug must flow out of and away from the conduit or must spread laterally within an underground cavity. The direct observations of the lava surface during gas pistoning at the Drainhole vent show that lateral spreading and subsequent thinning of the overlying magma were not necessary for the gas release phase of the gas pistons we documented to occur.

Edmonds and Gerlach (2007) used Fourier transform infrared spectroscopy to study the composition of gases emitted during a single outgassing burst at a different vent in Puʻu ʻŌʻō in 2004. They found that the transient event involved CO_2-rich gas that segregated at depth, implying the involvement of a gas slug. The event they document was one of two such events that occurred at that vent during 3 h of observation (M. Edmonds, written communication, 2009). Edmonds and Gerlach (2007) made their observation at an eruptive vent topped by a spatter cone. Thus, no direct view of the lava surface was possible. While similar in duration (~26 min) to the gas pistons we studied, the incandescence steadily brightened prior to the outgassing burst, exactly the opposite of the decreasing brightness observed at the Drainhole vent during gas pistoning. The decreasing brightness we observed is, however, consistent with the decreasing thermal levels during gas pistoning reported by Johnson et al. (2005) and Marchetti and Harris (2008), and it is similar to changes in brightness at Kīlauea's summit lava lake in 2008–2009 (Patrick et al. 2011a). Edmonds and Gerlach (2007) also report several minutes of low rumbling emanating from the vent, followed by several minutes of loud roaring. In contrast, Swanson et al. (1979) describe a quiet rise of the lava surface during gas pistoning, which matches our observations of gas piston activity at Puʻu ʻŌʻō at other times (gas pistoning during the deployment period was not observed during field visits). We agree with Patrick et al. (2011b) that the event studied by Edmonds and Gerlach (2007), though inferred by them to be a gas piston, probably represents some other type of sporadic gas release.

The slowing rate of lava level rise presented here is broadly similar in form to the pressure balance analog experiments of Witham et al. (2006), who streamed air through a vertical water-filled pipe to produce oscillations in the level of water in an overlying tank. The streaming air decreases the density of the water column, causing the water surface to rise. Bubbles continue to increase in size until instability is triggered and the water level drops. Though not explicitly stated, their experiment implies that bubbles continue to burst at the water surface as the water level rises. This is inconsistent with our observations, which show that the amount of gas streaming through the lava surface is reduced during the lava surface rise. In the absence of bubble bursting, the lava surface becomes encrusted, and vent incandescence is markedly reduced.

While rising gas slugs or a dynamic pressure balance are unlikely mechanisms for the gas pistons that we observed at the Drainhole vent, our results are consistent with a progressive shallow accumulation of gas. The study, though, does not specifically determine the process by which that gas accumulates. Swanson et al. (1979) suggested that gas was prevented from escaping by the brittle surface crust on the lava column. Using improved observations, Patrick et al.

(2011b) suggested that the viscoelastic layer beneath the surface crust was the true barrier. In either case, puncturing should result in the release of gas and the termination of the gas piston. Indeed, this was seen at Mauna Ulu where the termination of gas pistons could be triggered manually by tossing rocks onto the lava surface (Swanson et al. 1979). The gas release could be initiated at slightly earlier times by introducing an even larger artificial shock to the system (Swanson et al. 1979). Similarly, at Kīlauea's summit lava lake during 2010–2011, the collapse of gas pistons was often triggered by small rockfalls from the walls of the vent (Orr et al. 2010). The gas release, however, could be triggered only when the gas piston was already close to collapse anyway. These observations, combined with the slowing rate of surface rise, suggest a process more complex than the simple trapping and subsequent release of gas.

Such observations, however, can be explained if the gas is locked within a foam layer, as suggested by Dibble (1972). Though similar in minor ways to the collapsing-foam model of Jaupart and Vergniolle (1988), this foam layer, rather than forming beneath the roof of a magma chamber, is forming instead at the top of the lava column, where it acts as a rheological barrier. The decoupled flow of H_2O and SO_2 gas through low-viscosity basalt favors the formation of foam, and the slowing rise rate of gas pistons is readily explained by a foam layer approaching a critical thickness, where the addition of new bubbles is balanced by foam drainage and weak outgassing. The coalescence of bubbles as the foam evolves results in fewer, but larger, bubbles that are no longer able to support the weight of the foam layer. Eventually, unless triggered externally, spontaneous collapse of the foam structure occurs and the gas trapped within is released. The system is thus reset for the next gas piston to begin.

Conclusion

Direct observations of the lava surface during this study offered an exceptional view of gas piston activity and provided a way to measure changes in the level of the top of the lava column. We found that the duration of the lava rise ranged from 2 to 60 min and, importantly, that the rate of rise slowed with time. There was, in general, a linear relation between gas piston volume and duration, but the time delay between successive pistons was not obviously dependent on the gas piston rise duration. Also, the gas release phase lasted, on average, 49 s. The commencement of the gas release phase occurred without requiring that the lava surface spread laterally, either by flowing out of the vent conduit or into a subterranean cavity.

Taken together, our results show that the gas slug and pressure balance models are unlikely mechanisms for the gas pistons that we observed at the Drainhole vent. Our results, however, are consistent with both the crust-controlled gas accumulation model as originally proposed by Swanson et al. (1971, 1979) and the foam model of Dibble (1972). We favor the model of Dibble (1972) which suggests that the gas accumulation takes the form of the generation (and collapse) of a foam layer at the top of the lava column. The main distinction between these two gas accumulation models is that, in the foam model, the formation of a relatively stable crust at the top of the lava column during gas pistoning is the consequence and not the cause of the gas accumulation, as was proposed by Swanson et al. (1979). The foam itself is a rheological barrier, and its formation allows a surface crust to develop and prevents that crust from being continually disrupted by inhibiting outgassing.

Because our observations of gas pistoning are essentially identical to the descriptions of the multitude of other directly observed gas pistons at Kīlauea, and are consistent with those of Swanson et al. (1979), Patrick et al. (2011a), and Patrick et al. (2011b), we believe that our results can be extended to gas piston activity at Kīlauea in general, regardless of vent location. Furthermore, the shallow generation and destruction of a foam layer may be manifested in ways different than gas pistoning and could control other types of degassing behavior at open-vent basaltic systems like Kīlauea.

Acknowledgments We gratefully thank Hawaiian Volcano Observatory staff and volunteers for field support, observations, and discussions about gas piston processes. Paul Wessel at University of Hawai'i at Mānoa provided the statistical analysis of gas release durations, for which we are appreciative. Careful and constructive reviews by Bruce Houghton, Dave Sherrod, Mike James, and Letizia Spampinato improved the manuscript greatly.

Appendix

The position of the lava surface within the Drainhole vent is calculated by re-projecting the lava surface from the image plane to the vertical plain defined by the vent wall. To achieve this, we first calculate the time-lapse camera's angular field of view, or angle of view (AOV), in the vertical direction using the equation:

$$\alpha = 2 \cdot \tan^{-1}\left(\frac{d}{2f}\right) \quad (1)$$

where α represents the vertical AOV, d represents the size of the camera's optical sensor in the vertical direction (5.32 mm for digital cameras with a 1/1.8″ optical sensor), and f represents the focal length (8.0 mm; obtained from image metadata). Solving for α, we find the camera's vertical AOV to be 36.8°. The same value was achieved when calculating vertical AOV directly from photographs of a flat object (the side of a building) of known size and distance from the camera. We ignore the radial distortion of the camera lens because our object of interest—the rising and falling lava surface—is near the center of the image, where radial distortion is negligible.

The inclination of the camera and the horizontal distance from the camera to the targeted vent wall defines a right triangle (Fig. 6a; in gray). From this, we use the cosine function for a right triangle to calculate a length of 12 m for the FOV center line, or principal ray (Fig. 6a; dashed red line). We also know that the acute angle formed by the intersection of the projected image plane and the vertical plane is equivalent to the inclination of the camera (26°) because it is complementary to the angle between the camera's principal ray and the vertical plane. To find the relative vertical position of the lava surface in any time-lapse image, we must imagine a line extending from the camera to the point of intersection between the lava surface and the vent wall. We refer to this line as the target ray (Fig. 6b; dashed blue line). When the slope of the target ray is steeper than that of the principal ray, the target ray passes through the projected image plane. We can then ratio the number of vertical pixels that comprise the segment of the projected image plane between the principal ray and the target ray (Fig. 6b; solid blue line) to the number of pixels that comprise half the vertical image frame (600 pixels). Cross-multiplying this with 18.5° (half of the AOV) gives us the angle between the principal ray and the target ray. The tangent function for a right triangle can then be used to calculate the length of the projected image plane between the principal ray and the target ray (Fig. 6b; solid blue line).

We now define a new triangle bounded by the projected image plane, the vertical vent wall, and the target ray (Fig. 6b). For this triangle, the angle between the projected image plane and the vent wall is 26°, and the angle between the projected image plane and the target ray is a supplementary angle and can be readily calculated. Since we now know two angles and the length of the included side, we use the law of sines to find the length of the side that represents the level of the lava surface in the vertical plane (Fig. 6b; solid green line). Using a variation of this procedure, we calculate the vertical distance between the principal ray of the camera and the vent rim (because the principal ray was below the vent rim). We then add this value to our calculated measurement of the lava level below the principal ray to get the total distance from the vent rim to the lava surface.

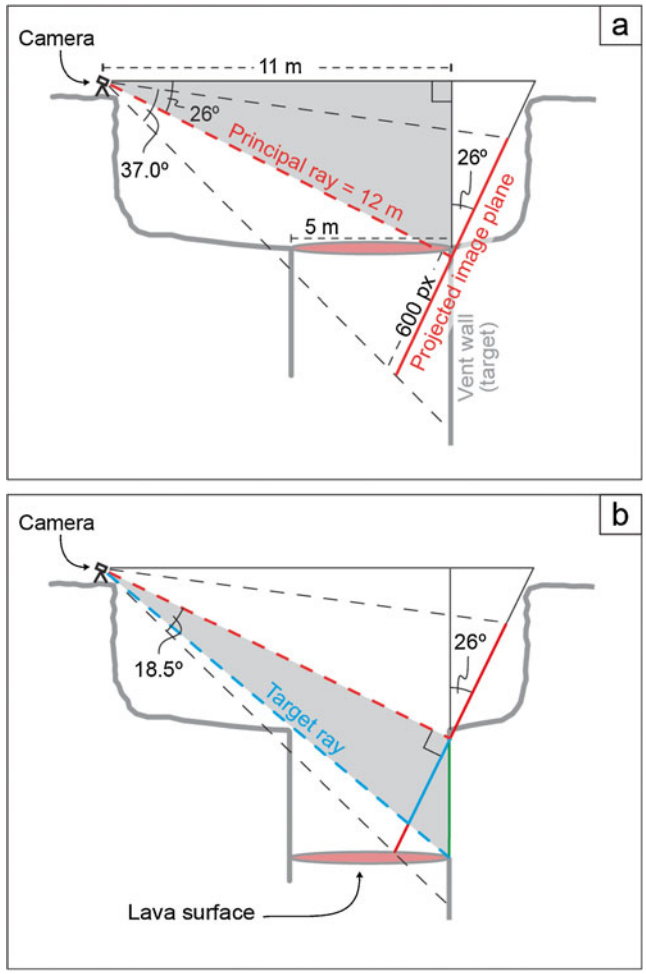

Fig. 6 Illustrations showing geometric details of time-lapse camera deployment at Drainhole vent. **a** Horizontal distance from camera to target (opposite wall of inner vent opening) is 11 m. *Black dashed lines* bound camera's field of view; *red dashed line* represents camera's principal ray, calculated length 12 m; *red solid line*, normal to principal ray, represents plane of projected image. **b** *Black dashed lines* bound camera's field of view; *red dashed line* represents camera's principal ray; *blue dashed line* represents target ray. Principal ray bisects projected image plane into upper and lower halves of 600 pixels each. Projected lava surface height represented by *solid blue line*; actual lava surface level represented by *solid green line*

This procedure is used to determine the position of the lava surface within the vent only when the surface is below the principal ray. A variation on this procedure is used when the lava surface rises above the camera's principal ray. Inaccuracy in the inclination of the camera and the distance between the camera and the targeted vent or pit wall will lead to small errors in the calculated height of the lava surface, as will small errors in the value calculated for the camera's angle of view. However, since the viewing geometry does not change from image to image, and because it is the relative change in the position of the lava surface that is important, we make no effort to quantify these errors and they are ignored.

References

Aster R, Mah S, Kyle P, McIntosh W, Dunbar N, Johnson J, Ruiz M, McNamara S (2003) Very long period oscillations of Mount Erebus Volcano. J Geophys Res 108(B11):2522. doi:10.1029/2002JB002101

Barker SR, Sherrod DR, Lisowski M, Heliker C, Nakata JS (2003) Correlation between lava-pond drainback, seismicity and ground deformation at Pu'u 'Ō'ō. In: Heliker C, Swanson DA, Takahashi TJ (eds) The Pu'u 'Ō'ō–Kupaianaha eruption of Kīlauea Volcano, Hawai'i: the first 20 years. US Geol Surv Prof Pap 1676: 53–62

Cashman KV, Mangan MT, Newman S (1994) Surface degassing and modifications to vesicle size distributions in active basalt flows. J Volcanol Geotherm Res 61(1–2):45–68

Dibble RR (1972) Seismic and related phenomena at active volcanoes in New Zealand, Hawaii, and Italy. PhD dissertation, Victoria University, Wellington

Dibble RR, Kyle PR, Rowe CA (2008) Video and seismic observations of Strombolian eruptions at Erebus volcano, Antarctica. J Volcanol Geotherm Res 177:619–634

Edmonds M, Gerlach TM (2007) Vapor segregation and loss in basaltic melts. Geology 35:751–754

Elias T, Sutton AJ (2007) Sulfur dioxide emission rates from Kilauea Volcano, Hawai'i, an update: 2002–2006. US Geol Surv Open-File Rep 2007-1114. http://pubs.usgs.gov/of/2007/1114/. Accessed 28 Aug 2012

Ferrazzini V, Aki K, Chouet B (1991) Characteristics of seismic waves composing Hawaiian volcanic tremor and gas-piston events observed by a near source array. J Geophys Res 96:6199–6209

Gerlach TM (1986) Exsolution of H_2O, CO_2, and S during eruptive episodes at Kilauea Volcano, Hawaii. J Geophys Res 91 (B12):12,177–112,185

Gerlach TM, Graeber EJ (1985) Volatile budget of Kilauea Volcano. Nature 313(6000):273–277

Gerst A, Hort M, Kyle PR, Vöge M (2008) 4D velocity of Strombolian eruptions and man-made explosions derived from multiple Doppler radar instruments. J Volcanol Geotherm Res 177:648–660

Heliker C, Mattox TN (2003) The first two decades of the Pu'u 'Ō'ō–Kupaianaha eruption: chronology and selected bibliography. In: Heliker C, Swanson DA, Takahashi TJ (eds) The Pu'u 'Ō'ō–Kupaianaha eruption of Kīlauea Volcano, Hawai'i: the first 20 years. US Geol Surv Prof Pap 1676: 1–27

Heliker CC, Mangan MT, Mattox TN, Kauahikaua JP, Helz RT (1998) The character of long-term eruptions: inferences from episodes 50–53 of the Pu'u 'Ō'ō–Kūpaianaha eruption of Kīlauea Volcano. Bull Volcanol 59(6):381–393

Heliker C, Kauahikaua J, Sherrod DR, Lisowski M, Cervelli P (2003) The rise and fall of Pu'u 'Ō'ō cone, 1983–2002. In: Heliker C, Swanson DA, Takahashi TJ (eds) The Pu'u 'Ō'ō–Kupaianaha eruption of Kīlauea Volcano, Hawai'i: the first 20 years. US Geol Surv Prof Pap 1676: 29–51

Hon K, Kauahikaua J, Denlinger R, Mackay K (1994) Emplacement and inflation of pahoehoe sheet flows: observations and measurements of active lava flows on Kilauea Volcano, Hawaii. Geol Soc Am Bull 106(3):351–370

James MR, Lane SJ, Corder SB (2008) Modelling the rapid near-surface expansion of gas slugs in low-viscosity magmas. In: Lane SJ, Gilbert JS (eds) Fluid motions in volcanic conduits: a source of seismic and acoustic signals. Geol Soc London Spec Publ 307: 147–167

Jaupart C, Vergniolle S (1988) Laboratory models of Hawaiian and Strombolian eruptions. Nature 331:58–60

Johnson JB, Harris AJL, Hoblitt RP (2005) Thermal observations of gas pistoning at Kilauea volcano. J Geophys Res 110:B11201. doi:10.1029/2005JB003944

Kauahikaua J, Mangan M, Heliker C, Mattox T (1996) A quantitative look at the demise of a basaltic vent: the death of Kupaianaha, Kilauea Volcano, Hawai'i. Bull Volcanol 57 (8):641–648

Marchetti E, Harris AJL (2008) Trends in activity at Pu'u 'O'o during 2001–2003: insights from the continuous thermal record. In: Lane SJ, Gilbert JS (eds) Fluid motions in volcanic conduits: a source of seismic and acoustic signals. Geol Soc London Spec Pub 307: 85–101

Mattox TN, Heliker C, Kauahikaua J, Hon K (1993) Development of the 1990 Kalapana flow field, Kilauea Volcano, Hawaii. Bull Volcanol 55(6):407–413

Orr T, Hoblitt RP (2008) A versatile time-lapse camera system developed by the Hawaiian Volcano Observatory for use at Kīlauea Volcano, Hawai'i. US Geol Surv Sci Invest Rept 2008-5117. http://pubs.usgs.gov/sir/2008/5117. Accessed 28 Aug 2012

Orr TR, Patrick MR, Wilson D, Sutton AJ, Elias T (2010) The impact of rockfalls on shallow degassing processes during the 2008–2010 summit eruption of Kīlauea Volcano, Hawai'i: Abstract #V21C-2340 presented at 2010 Fall Meeting, AGU, San Francisco, California, 13–17 Dec

Patrick MR, Harris AJL, Ripepe M, Dehn J, Rothery DA, Calvari S (2007) Strombolian explosive styles and source conditions: insights from thermal (FLIR) video. Bull Volcanol 69:769–784

Patrick MR, Kauahikaua JP, Antolik L (2010) MATLAB tools for improved characterization and quantification of volcanic incandescence in Webcam imagery: applications at Kīlauea Volcano, Hawai'i. US Geol Tech Method 13-A1. http://pubs.usgs.gov/tm/tm13a1/. Accessed 28 Aug 2012

Patrick M, Wilson D, Fee D, Orr T, Swanson D (2011a) Shallow degassing events as a trigger for very-long-period seismicity at Kīlauea Volcano, Hawai'i. Bull Volcanol 73(9):1179–1186

Patrick MR, Orr T, Wilson D, Dow D, Freeman R (2011b) Cyclic spattering, seismic tremor, and surface fluctuation within a perched lava channel, Kīlauea Volcano. Bull Volcanol 73 (6):639–653

Ripepe M, Marchetti E (2002) Array tracking of infrasonic sources at Stromboli volcano. Geophys Res Lett 29:2076. doi:10.1029/2002GL015452

Swanson DA, Jackson DB, Duffield WA, Peterson DW (1971) Mauna Ulu eruption, Kilauea Volcano. Geotimes 16(5):12–16

Swanson DA, Duffield WA, Jackson DB, Peterson DW (1979) Chronological narrative of the 1969–71 Mauna Ulu eruption of Kilauea volcano, Hawaii. US Geol Surv Prof Pap 1056

Tilling RI, Christiansen RL, Duffield WA, Endo ET, Holcomb RT, Koyanagi RY, Peterson DW, Unger JD (1987) The 1972–1974 Mauna Ulu eruption, Kilauea Volcano: an example of quasi-steady-state magma transfer. In: Decker RW, Wright TL, Stauffer PH (eds) Volcanism in Hawaii. US Geol Surv Prof Pap 1350, 2: 405–469

Vergniolle S, Mangan M (2000) Hawaiian and Strombolian eruptions. In: Sigurdsson H, Houghton BF, McNutt S, Rymer H, Stix J (eds) Encyclopedia of volcanoes. Academic, San Diego, pp 447–461

Witham F, Woods AW, Gladstone C (2006) An analogue experimental model of depth fluctuations in lava lakes. Bull Volcanol 69(1):51–56

Wolfe EW, Neal CA, Banks NG, Duggan TJ (1988) Geologic observations and chronology of eruptive events. In: Wolfe EW (ed) The Puu Oo eruption of Kilauea Volcano, Hawaii: episodes 1–20, January 3, 1983, through June 8, 1984. US Geol Surv Prof Pap 1463, 1–97